

## Supporting Information

Broadband near-infrared BaMSi<sub>3</sub>O<sub>9</sub>:Cr<sup>3+</sup> (M = Zr, Sn, Hf) phosphors for light-emitting diode applications

Yan Zhang, Yanjie Liang,\* Shihai Miao, Dongxun Chen, Shao Yan and Jingwei Liu

Key Laboratory for Liquid-Solid Structure Evolution and Processing of Materials,

Ministry of Education, Shandong University, Jinan 250061, P. R. China

\*Corresponding author: YJ Liang

E-mail: yanjie.liang@sdu.edu.cn

## Contents

<b>1. Figures.....</b>	<b>3</b>
Fig. S1 (a) Emission spectra of BaMSi <sub>3</sub> O <sub>9</sub> :Cr <sup>3+</sup> (M = Zr, Sn, Hf) phosphors as a function of Cr <sup>3+</sup> doping concentration.....	3
Fig. S2 Diffuse reflectance spectra of BaMSi <sub>3</sub> O <sub>9</sub> :Cr <sup>3+</sup> phosphors.....	4
Fig. S3 Excitation line of BaSO <sub>4</sub> and emission spectra of the BaMSi <sub>3</sub> O <sub>9</sub> :Cr <sup>3+</sup> (M = Zr, Sn, Hf) phosphors collected using an integrating sphere.....	5
Fig. S4 Photoelectric conversion efficiency of the NIR LED fabricated by BaSnSi <sub>3</sub> O <sub>9</sub> :Cr <sup>3+</sup> phosphor.....	6
Fig. S5 (a) Electroluminescence spectra of the NIR LED fabricated by BaHfSi <sub>3</sub> O <sub>9</sub> :Cr <sup>3+</sup> phosphor and blue LED chip under various drive currents. (b) NIR output power of the LED device under various drive currents. (c) Photoelectric conversion efficiency as a function of drive currents.....	7
<b>2. Tables.....</b>	<b>8</b>
Table. S1 Photoluminescence properties of Cr <sup>3+</sup> in different host materials.....	8
Table. S2 ICP analysis of Cr content in BaMSi <sub>3</sub> O <sub>9</sub> (M = Zr, Sn, Hf) samples.....	9
Table. S3 The output power and photoelectric conversion efficiency of blue LED chip at different drive currents.....	10
<b>3. Reference.....</b>	<b>11</b>

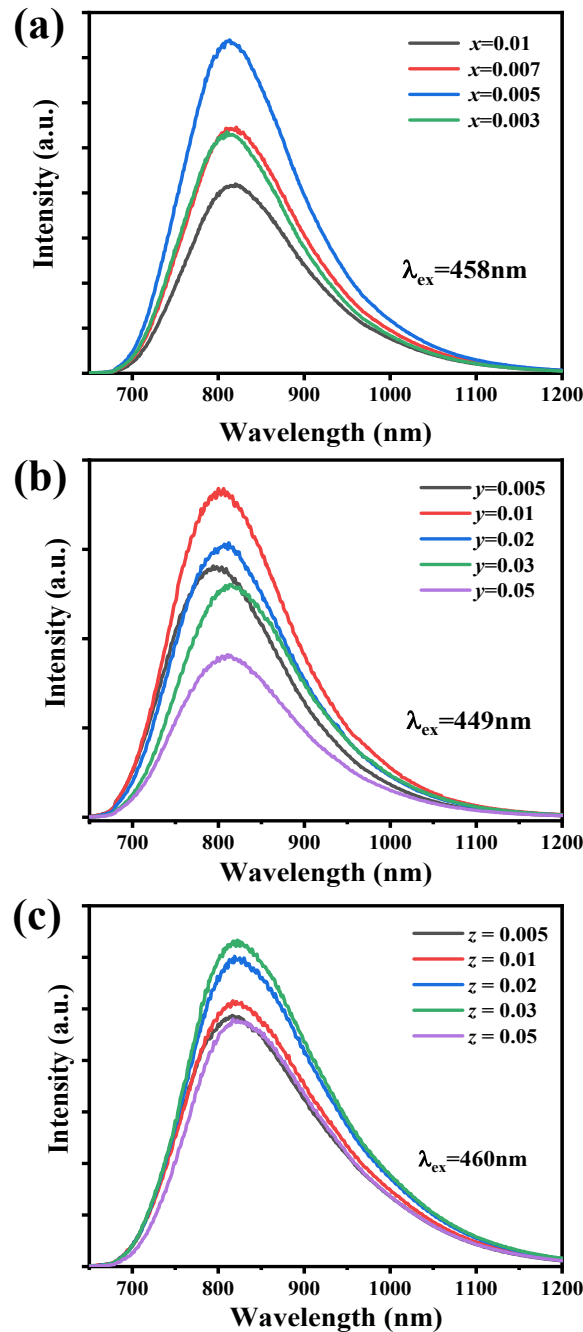


**Fig. S1** (a) Emission spectra of  $\text{BaZr}_{1-x}\text{Si}_3\text{O}_9:x\text{Cr}^{3+}$  ( $x = 0.003, 0.005, 0.007, 0.01$ ) phosphor at room temperature. (b, c) Emission spectra of  $\text{BaSn}_{1-y}\text{Si}_3\text{O}_9:y\text{Cr}^{3+}$  and  $\text{BaHf}_{1-z}\text{Si}_3\text{O}_9:z\text{Cr}^{3+}$  ( $y, z = 0.005, 0.01, 0.02, 0.03$  and  $0.05$ ) phosphors at room temperature.

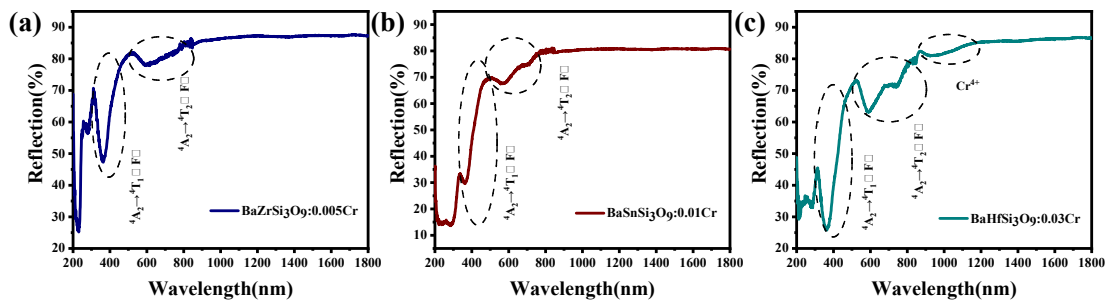


**Fig. S2** Diffuse reflectance spectra of BaMSi<sub>3</sub>O<sub>9</sub>:Cr<sup>3+</sup> (M = Zr, Sn, Hf) phosphors.

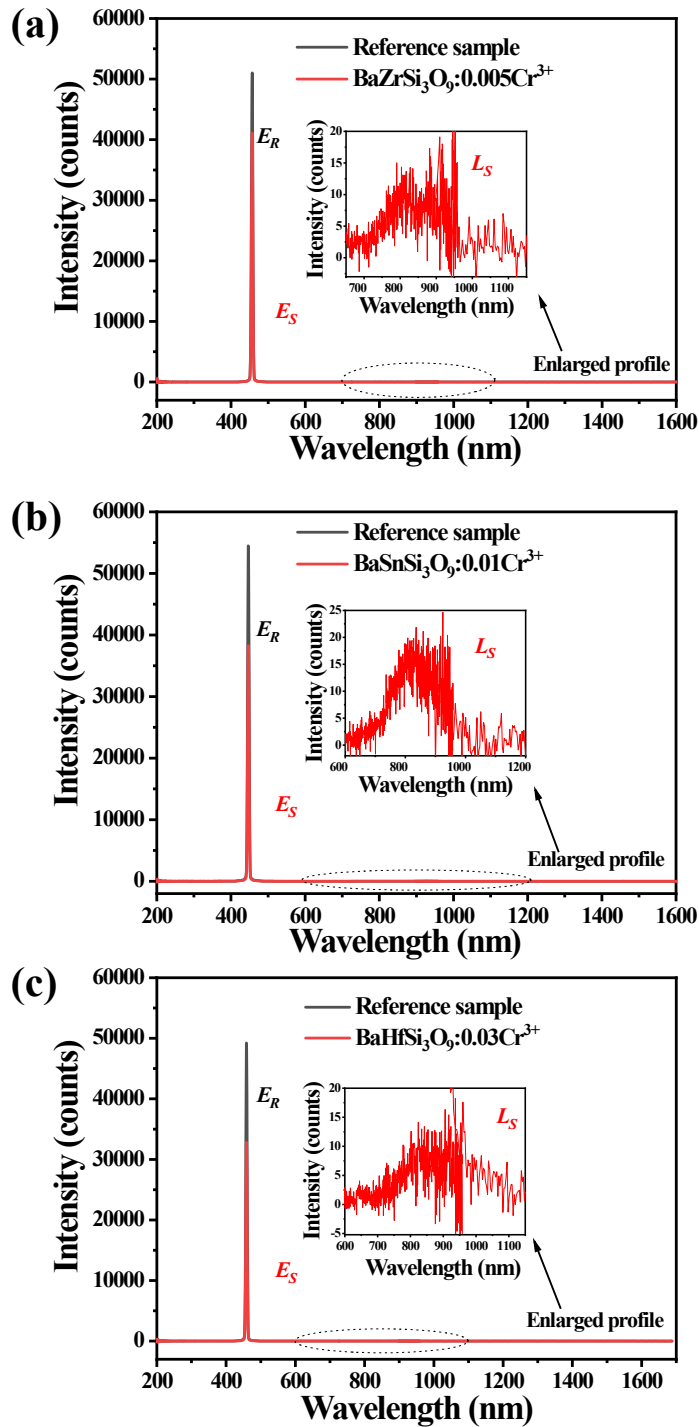


**Fig. S3** Excitation line of  $\text{BaSO}_4$  and emission spectrum of the selected  $\text{BaMSi}_3\text{O}_9:\text{Cr}^{3+}$  ( $\text{M} = \text{Zr}, \text{Sn}, \text{Hf}$ ) phosphors collected using an integrating sphere. The inset shows a magnification of the emission spectrum. The measured internal quantum efficiencies of  $\text{BaMSi}_3\text{O}_9:\text{Cr}^{3+}$  phosphors are determined to be 7% ( $\text{BaZrSi}_3\text{O}_9:0.5\%\text{Cr}^{3+}$ ), 16% ( $\text{BaSnSi}_3\text{O}_9:1\%\text{Cr}^{3+}$ ) and 13% ( $\text{BaHfSi}_3\text{O}_9:3\%\text{Cr}^{3+}$ ), respectively.

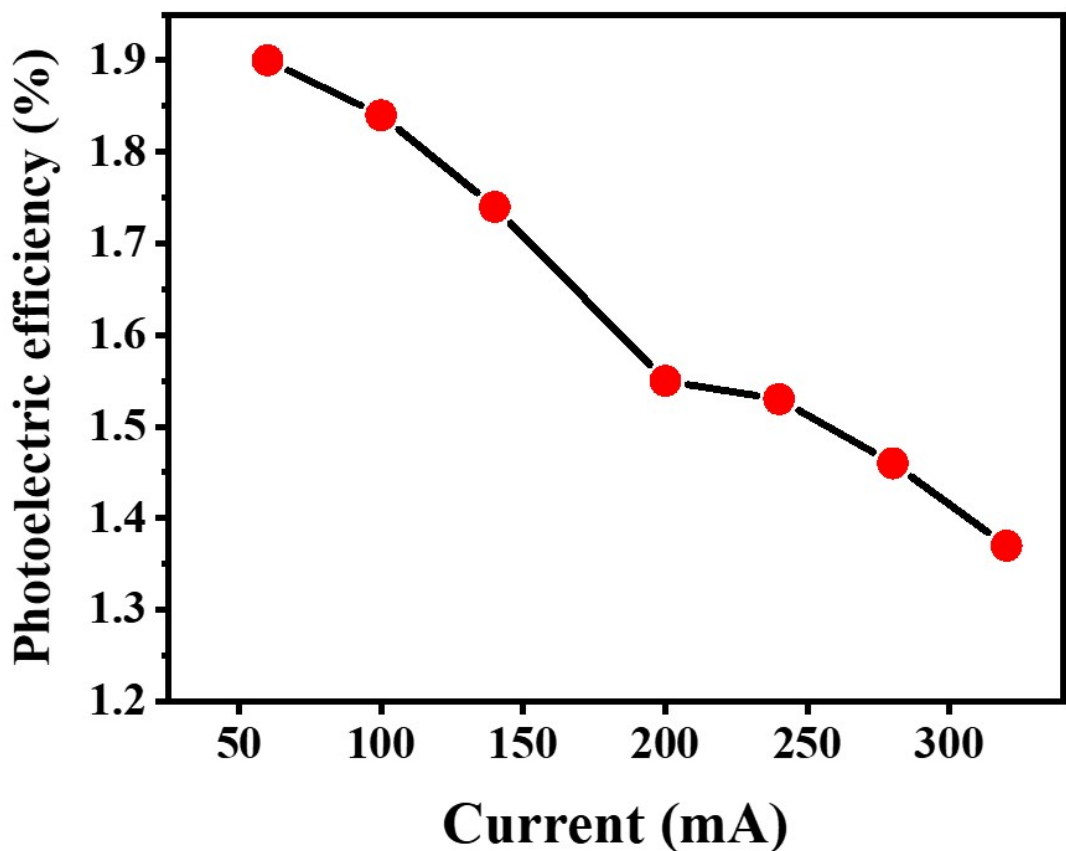
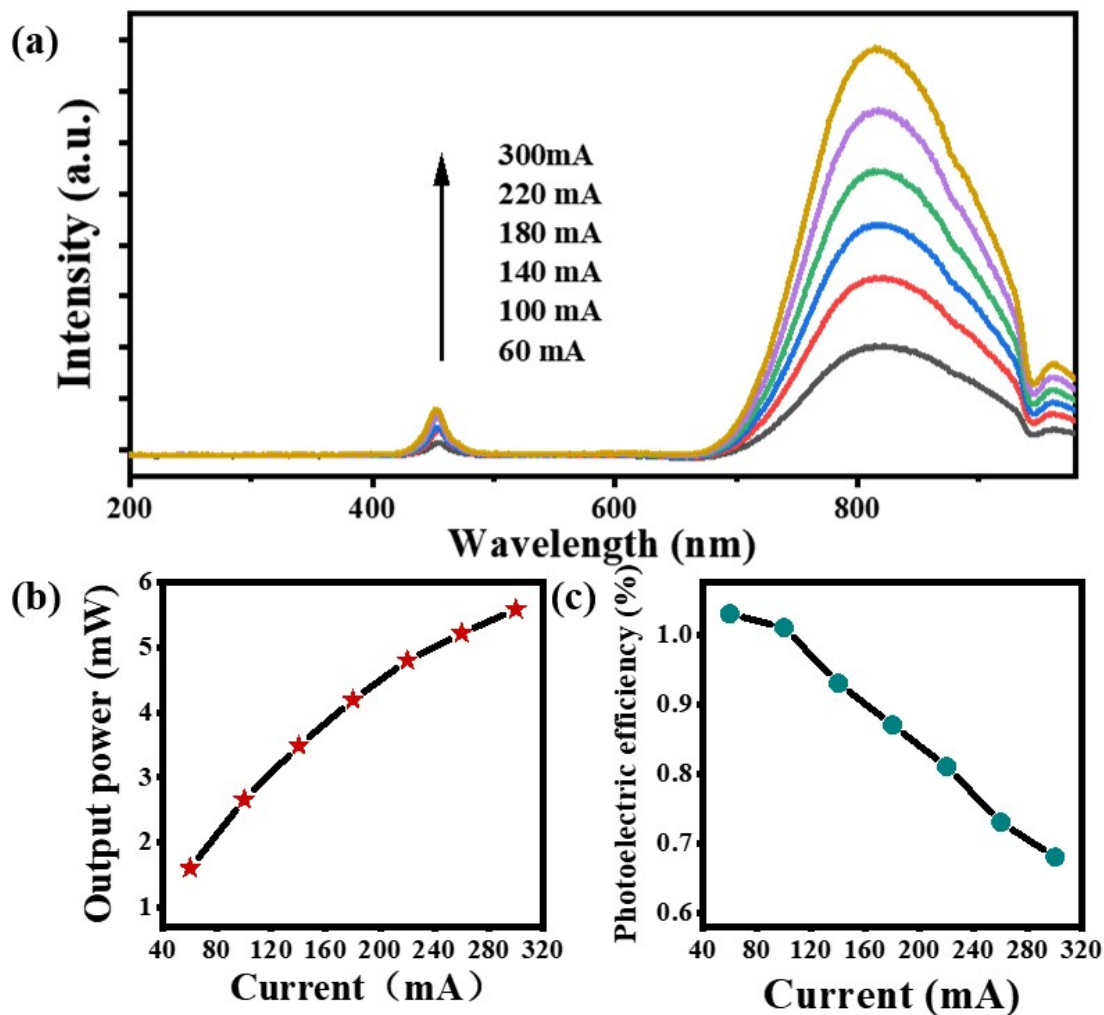


Fig. S4 Photoelectric conversion efficiency of the NIR LED fabricated by BaSnSi<sub>3</sub>O<sub>9</sub>:Cr<sup>3+</sup> phosphor



**Fig. S5** (a) Electroluminescence spectra of the NIR LED fabricated by  $\text{BaHfSi}_3\text{O}_9:\text{Cr}^{3+}$  phosphor and blue LED chip under various drive currents. (b) NIR output power of the LED device under various drive currents. (c) Photoelectric conversion efficiency as a function of drive currents.

**Table S1** Photoluminescence properties of Cr<sup>3+</sup> in different host materials

<b>Cr<sup>3+</sup> doped phosphor</b>	<b>λ<sub>exc</sub>(nm)</b>	<b>λ<sub>em</sub>(nm)</b>	<b>FWHM(nm)</b>	<b>refs</b>
Gd <sub>3</sub> Sc <sub>2</sub> Ga <sub>3</sub> O <sub>12</sub> :Cr	460	754	90	1
Lu <sub>3</sub> Sc <sub>2</sub> Ga <sub>3</sub> O <sub>12</sub> :Cr	446	772	73	1
Y <sub>3</sub> Ga <sub>5</sub> O <sub>12</sub> :Cr	442	710	85	2
Gd <sub>3</sub> Ga <sub>5</sub> O <sub>12</sub> :0.05Cr	447	717	~90	2
Gd <sub>3</sub> Sc <sub>1.5</sub> Al <sub>0.5</sub> Ga <sub>3</sub> O <sub>12</sub> :Cr	460	756	120	3
Ca <sub>2</sub> LuZr <sub>2</sub> Al <sub>3</sub> O <sub>12</sub> :0.08Cr	460	752	117	4
Ca <sub>3</sub> Sc <sub>2</sub> Si <sub>3</sub> O <sub>12</sub> : Cr	460	770	~110	5
Y <sub>2</sub> CaAl <sub>4</sub> SiO <sub>12</sub> :0.006 Cr	440	744	160	6
Na <sub>3</sub> Al <sub>2</sub> Li <sub>3</sub> F <sub>12</sub> :0.05Cr	430	750	~110	7
CaLu <sub>2</sub> Mg <sub>2</sub> Si <sub>3</sub> O <sub>12</sub> :Cr	445	765	120	8
Ca <sub>3</sub> Y <sub>2</sub> Ge <sub>3</sub> O <sub>12</sub> :Cr	460	800	110	9
BaZrSi <sub>3</sub> O <sub>9</sub> :0.005Cr	458	811	155	This work
BaSnSi <sub>3</sub> O <sub>9</sub> :0.01Cr	449	806	162	This work
BaHfSi <sub>3</sub> O <sub>9</sub> :0.03Cr	460	822	184	This work

**Table S2 The ICP analysis of Cr content in BaMSi<sub>3</sub>O<sub>9</sub> samples.**

Sample	Element	Sample weight/g	Solution volume/ml	Dilution factor	Test Indicating value/mg/L	Element concentration/mg/kg	Element mole fraction/mol%
BaZrSi <sub>3</sub> O <sub>9</sub> ;0.5%Cr <sup>3+</sup>	Cr	0.151	50	1	1.4451	478.816	0.42
BaSnSi <sub>3</sub> O <sub>9</sub> ;1%Cr <sup>3+</sup>	Cr	0.149	50	1	2.0143	676.3842	0.63
BaHfSi <sub>3</sub> O <sub>9</sub> ;3%Cr <sup>3+</sup>	Cr	0.168	50	1	2.2890	682.8819	0.71

**Table S3 The output power and photoelectric conversion efficiency of blue LED chip at different drive currents.**

<b>Drive currents(mA)</b>	<b>Input power(mW)</b>	<b>Output power (mW)</b>	<b>Photoelectric efficiency (%)</b>
20	53.1	30.9	56.57
60	168.2	93.9	57.39
100	299.6	155.5	57.00
140	437.0	215.5	56.36
180	577.0	272.9	55.50
220	705.3	329.5	54.80
240	770.7	357.5	54.50
260	840.4	385.0	54.17
280	908.9	411.8	53.81
300	976.0	438.9	53.46

## Reference

- [1] B. Malysa, A. Meijerink and T. Jüstel, Temperature dependent Cr<sup>3+</sup> photoluminescence in garnets of the type X<sub>3</sub>Sc<sub>2</sub>Ga<sub>3</sub>O<sub>12</sub> (X = Lu, Y, Gd, La), *J. Lumin.*, 2018, **202**, 523-531.
- [2] A. Zabiliute, S. Butkute, A. Zukauskas, P. Vitta and A. Kareiva, Sol-gel synthesized far-red chromium-doped garnet phosphors for phosphor-conversion light-emitting diodes that meet the photomorphogenetic needs of plants, *Appl. Opt.*, 2014, **53**, 907-914.
- [3] E. T. Basore, W. Xiao, X. Liu, J. Wu and J. Qiu, Broadband near-infrared garnet phosphors with near-unity internal quantum efficiency, *Adv. Opt. Mater.*, 2020, **8**, 200296.
- [4] L. Zhang, S. Zhang, Z. Hao, X. Zhang, G. Pan, Y. Luo, H. Wu and J. Zhang, A high efficiency broad-band near-infrared Ca<sub>2</sub>LuZr<sub>2</sub>Al<sub>3</sub>O<sub>12</sub>:Cr<sup>3+</sup> garnet phosphor for blue LED chips, *J. Mater. Chem. C*, 2018, **6**, 4967-4976.
- [5] Z. Jia, C. Yuan, R. Li, P. Sun, R. Dong, Y. Liu, L. Wang, H. Jiang and J. Jiang, Electron–phonon coupling mechanisms of broadband near-infrared emissions from Cr<sup>3+</sup> in the Ca<sub>3</sub>Sc<sub>2</sub>Si<sub>3</sub>O<sub>12</sub> garnet, *Phys. Chem. Chem. Phys.*, 2020, **22**, 10343-10350.
- [6] M. Q. Mao, T. L. Zhou, H. T. Zeng, L. Wang, F. Huang, X. Y. Tang and R. J. Xie, Broadband near-infrared (NIR) emission realized by the crystal-field engineering of Y<sub>3-x</sub>Ca<sub>x</sub>Al<sub>5-x</sub>Si<sub>x</sub>O<sub>12</sub>:Cr<sup>3+</sup> (x = 0–2.0) garnet phosphors, *J. Mater. Chem. C*, 2020, **8**, 1981-1988.
- [7] D. Huang, S. Liang, D. Chen, J. Hu, K. Xu and H. Zhu, An efficient garnet-structured Na<sub>3</sub>Al<sub>2</sub>Li<sub>3</sub>F<sub>12</sub>:Cr<sup>3+</sup> phosphor with excellent photoluminescence thermal stability for near-infrared LEDs, *Chem. Eng. J.*, 2021, **426**, 131332.
- [8] R. Li, Y. Liu, C. Yuan, G. Leniec, L. Miao, P. Sun, Z. Liu, Z. Luo, R. Dong and J. Jiang, Thermally Stable CaLu<sub>2</sub>Mg<sub>2</sub>Si<sub>3</sub>O<sub>12</sub>:Cr<sup>3+</sup> Phosphors for NIR LEDs, *Adv. Opt. Mater.*, 2021, **9**, 2100388.
- [9] N. Mao, S. Liu, Z. Song, Y. Yu and Q. Liu, A broadband near-infrared phosphor Ca<sub>3</sub>Y<sub>2</sub>Ge<sub>3</sub>O<sub>12</sub>:Cr<sup>3+</sup> with garnet structure, *J. Alloys Compd.*, 2021, **863**, 158699.